Salvador, FJ.; De La Morena, J.; Carreres, M.; Jaramillo-Císcar, D. (2017). Numerical analysis of flow characteristics in diesel injectors nozzles with convergent-divergent orifices. Proceedings of the Institution of Mechanical Engineers Part D Journal of Automobile Engineering. 231(14):1935-1944. doi:10.1177/0954407017692220

Numerical analysis of flow characteristics in diesel injector nozzles with convergent-divergent orifices.

Proceedings of the Institution of Mechanical Engineers, Part D: Journal of Automobile Engineering
XX(X):2–24

DOI: 10.1177/ToBeAssigned
www.sagepub.com/
SAGE

F.J. Salvador, J. De la Morena, M. Carreres and D. Jaramillo

Abstract

The geometry of diesel injector nozzles is known to significantly affect the characteristic spray behavior and emissions formation. In this paper, a novel nozzle concept, consisting on orifices with convergent-divergent shape, is investigated through CFD techniques. Three of these nozzles, characterized by different degrees of conicity, are compared to a nozzle with cylindrical orifices, which acts as a baseline. An Homogeneous Equilibrium Model (HEM), validated against experimental data in previous works by the authors, is used to calculate the eventual cavitation formation inside these orifices. Additionally, the characteristics of the flow at the orifice outlet are analyzed for the four aforementioned nozzles in terms of their stationary mass flow, effective outlet velocity and area coefficient. The results show that convergent-divergent nozzles exhibit high cavitation intensity, located in the transition between the convergent and the divergent sections. This high cavitation intensity tends to compensate for the expected velocity decrease induced by the divergent shape, producing effective velocity values similar to those achieved by the cylindrical nozzle in many of the simulated conditions. The characteristics of the flow, together with the higher spray opening angles expected due to the divergent section of the nozzle, may improve atomization and fuel-air mixing processes.

Keywords
nozzle,diesel,injection,CFD,cavitation,convergent-divergent

Nomenclature

ΔP	Pressure drop along the nozzle orifice
γ	Void fraction
μ	Fluid viscosity
μ_l	Liquid fuel viscosity
μ_v	Vapor fuel viscosity
Ψ	Fluid compressibility
Ψ_l	Liquid fuel compressibility
Ψ_v	Vapor fuel compressibility
ρ	Fluid density
$\rho_{l,sat}$	Saturated liquid fuel density
ρ_l	Liquid fuel density
$\rho_{v,sat}$	Saturated vapor fuel density
A_{eff}	Nozzle orifice outlet effective area
c	Speed of sound
C_a	Nozzle orifice area coefficient
C_d	Nozzle orifice discharge coefficient

CMT Motores Térmicos, Universitat Politècnica de València

Corresponding author:
F.J. Salvador CMT Motores Térmicos
Universitat Politècnica de València
Camino de Vera s/n
46022 Valencia (Spain)
Email: fsalvado@mot.upv.es

Prepared using sagej.cls *[Version: 2015/06/09 v1.01]*

C_v Nozzle orifice velocity coefficient

D_i Nozzle orifice inlet diameter

D_m Nozzle orifice outlet at the middle/throttle section

D_o Nozzle orifice outlet diameter

DPF Diesel Particulate Filter

EGR Exhaust Gas Recirculation

$k - factor$ Nozzle orifice conicity factor

LNT Lean NO_x Trap

$\dot{M}_o$ Nozzle orifice outlet momentum flux

$\dot{m}_o$ Nozzle orifice outlet mass flow rate

P Pressure

P_b Backpressure

P_{in} Injection pressure

P_{sat} Saturation pressure

SCR Selective Catalytic Reduction

u_{eff} Nozzle orifice outlet effective velocity

u_{th} Nozzle orifice theoretical outlet velocity, according to Bernoulli equation

Introduction

In the latest years, the implementation of new regulations have driven for a continuous optimization of engine technology in order to cope with the reduction on tailpipe emissions[1]. In the particular case of diesel engines, where combustion efficiencies are high, the main concern is set on NO_x and particulate matter (soot) emissions. Two main research paths have been pursued: on the one hand, aftertreatment systems combining a Diesel Particulate Filter (DPF) and, at least, one deNO_x component (such as Selective Catalytic Reduction -SCR- or Lean NO_x Trap -LNT-) have become mainstream on

diesel automotive application[2]. On the other hand, a significant effort has also been made to lower engine-out emissions. In this sense, Exhaust Gas Recirculation (EGR) has proven to be able to reduce NO_x emissions, but at the expense of increasing soot, unless combined with extreme levels of intake pressure[3–5]. Thus, an evolution of the fuel injection system, aiming at improving spray atomization and fuel-air mixing, is necessary to compensate for this increase and enable high EGR levels.

Many studies have shown that the injector nozzle geometry and its internal flow characteristics play a significant role on the spray formation[6–10] and combustion[11–14]. Traditionally, internal flow characteristics have been deduced from measurements of the flow characteristics at the nozzle outlet[15–17]. Cavitation inside the nozzle was identified as a critical phenomenon, inducing a decrease in the flow capacity of the nozzle, but also an increase in the spray outlet effective velocity[18]. The appearance of cavitation has also been linked to an enhancement of atomization process[19] and fuel-air mixing, inducing higher spray opening angles[20–22].

Several authors[23–26] have also performed visualization studies on transparent nozzles, aimed at better understanding the details of the cavitation structures and their dependence on the nozzle geometry and the operating conditions. Unfortunately, most of these studies are performed in scaled-up[20;25;28] or simplified nozzles[24;26], due to difficulties associated to both manufacturing and optical arrangement in realistic geometries. For this reason, computational fluid-dynamics tools have been developed as a methodology to obtain detailed characteristics of the internal flow features[27;29–34].

In the current paper, a novel diesel nozzle concept including orifices with convergent-divergent shape is evaluated using CFD simulations. In this case, the divergent section is expected to induce velocity profiles at the nozzle outlet with a significant radial component, increasing the spray opening angle and fuel-air mixing processes compared to traditional cylindrical or tapered orifices. The larger spray angle would imply, on the one hand, leaner local equivalence ratios, with the subsequent expected reduction in soot formation, and on the other hand, the possibility to develop the spray combustion closer to the nozzle tip, reducing heat transfer losses to the combustion chamber walls. Taskiran and Ergeneman[35] evidenced this behavior on a nozzle with divergent orifices, with a reduction in liquid length and lift-off length. Nevertheless, purely divergent orifices act as a diffuser, so lower outlet velocities are expected, with negative impact on spray atomization[36]. A Homogeneous Equilibrium Model (HEM), previously validated[37–39], is used to calculate the eventual appearance of hydrodynamic cavitation inside these nozzles.

The paper is divided in four sections. In section 2, the basics of the numerical approach used along the paper will be described. Section 3 will go through the analysis of the internal flow characteristics of a total of four nozzle geometries, including one cylindrical and other three with convergent-divergent shape at different degrees of conicity. Finally, the main conclusions obtained out of the study will be summarized in Section 4.

Numerical simulations description

In this section, the most significant aspects of the model implemented in OpenFoam and used along the paper, together with a description of the specific nozzle geometries studied, are summarized. More details of the specifics of the computational models can be obtained in previous publications by the authors[33;38–40].

Homogeneous Equilibrium Model

In the previous works available in the literature[30;33;40], Homogeneous Equilibrium Model (HEM) approach has shown to be suitable for studying cavitation phenomena in diesel injectors, due to the combination of high pressure and velocity gradients inside the flow. Compared to other models available in the literature, which track the formation and growth of cavitation bubbles, HEM assumes a full mixture of vapor and liquid phases inside each cell of the domain. The density of this mixture is computed using the following barotropic equation of state:

$$\left(\frac{\partial \rho\left(t, P(\vec{x}, t)\right)}{\partial P}\right)_t = \Psi = \frac{1}{c^2} \tag{1}$$

Once the mixture density is known, the amount of vapor present on each cell can be calculated using the concept of void fraction γ as:

$$\gamma = max\left(min\left(\frac{\rho - \rho_{l,sat}}{\rho_{v,sat} - \rho_{l,sat}}, 1\right), 0\right) \tag{2}$$

The major physical properties of the mixture (compressibility, density and viscosity) are derived from the values corresponding to pure liquid and vapor conditions using linear models:

$$\Psi = \gamma\Psi_v + (1-\gamma)\Psi_l \tag{3}$$

$$\rho = (1-\gamma)\rho_l^0 + \Psi \cdot P \tag{4}$$

$$\mu = \gamma\mu_v + (1-\gamma)\mu_l \tag{5}$$

Continuity and momentum conservation equations are discretized using in both cases Euler schemes for the temporal derivatives and Gauss upwind schemes for the divergence terms.

Turbulence model

The simulations performed along the paper are based on a Reynolds Average Navier-Stokes (RANS) approach, which has shown to provide a good representation of the average flow fields at limited computational cost. In particular, a Re-Normalization Groups (RNG) $k-\epsilon$ model has been implemented. This selection has been done attending to the flow characteristics inside diesel injector nozzles. First, the wide range of injection pressures currently used in diesel applications (from 30 MPa to around 200 MPa) implies a significant range in operating Reynolds numbers in the nozzle. Second, the small size of the nozzle orifices may result in the near wall effects having a significant influence of the overall flow characteristics. Finally, the flow in multi-hole diesel injectors suffers from aggressive changes in direction, generating flow detachment and recirculation regions. All these characteristics are typically better represented with RNG $k-\epsilon$ models compared to standard $k-\epsilon$ or $k-\omega$ methods.

The suitability of this approach has additionally been validated against experimental data in previous studies[38–41].

Nozzle geometries

Four different nozzle geometries have been computed for the study. The first one corresponds to a cylindrical orifice. The other three are convergent-divergent nozzles (see schematic at Figure 1.a) at different levels of conicity, characterized by taper angles of 0.5, 2.5 and 3.5 degrees, equal for both the convergent and divergent the sections. As a consequence, the nozzles show different values of the so-called $k-factor$, defined as:

$$k-factor = \frac{D_i - D_o}{10[\mu\text{m}]} \tag{6}$$

As stated before, the same level of conicity has been used for the convergent and divergent sections, so the absolute value of $k-factor$ is also equal. This implies a positive $k-factor$ for the convergent section, and a negative $k-factor$ for the divergent.

The transition between the convergent and divergent regions always takes place at the middle of the orifice length (0.8 mm). Additionally, the nozzle geometries have been constructed so that the orifice diameter at this throttle/transition section (D_m) is maintained equal to the outlet diameter of the cylindrical nozzle. The representative diameters and conicity values for each of the nozzles are summarized in Table 1. Other geometrical parameters of the nozzles are maintained constant for all the nozzles. In particular, the inclination of the orifices with respect to the injector axis is 72.5 degrees, and the rounding radius at the orifice inlet is 0.025 mm .

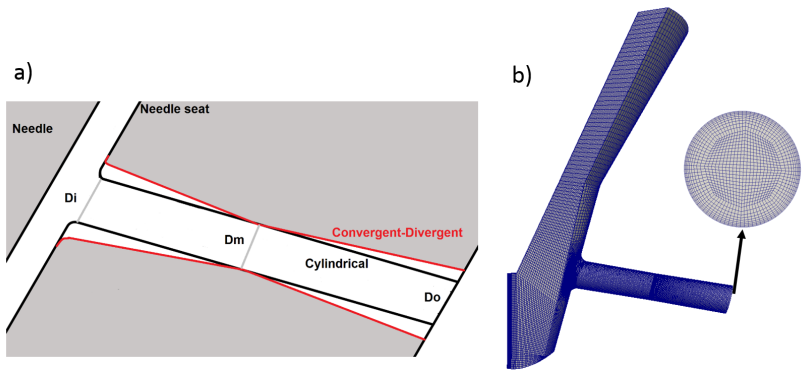

Figure 1. a) Nozzle geometry schematic. b) Detail of mesh topology.

Table 1. Geometrical characteristics of the nozzles tested.

Nozzle	Angle [°]	$k-factor$ [-]	D_i [mm]	D_m [mm]	D_o [mm]
CD0.0	0	0	0.125	0.125	0.125
CD0.5	0.5	0.6	0.131	0.125	0.131
CD2.5	2.5	3.1	0.156	0.125	0.156
CD3.5	3.5	4.4	0.169	0.125	0.169

Mesh topology and boundary conditions

For all the geometries studied, the mesh has been generated using hexahedral cells, trying to maintain a uniform and structured distribution of these cells along the computational

domain. The cell size has been also adapted according to the flow characteristics inside each region. A mesh sensitivity study has been done to select the most appropriate cells size (Figure 2). From this study, the configuration of approximately 377000 cells has been selected. For the needle seat and sac volume, typically characterized by low velocity and organized flow, a uniform size of 22.5 µm has been used. Inside the nozzle orifices, where the maximum velocities are reached, the cell size has been reduced to around 7 µm. Additionally, the mesh has been refined up to 1.15 µm close to the walls of these orifices, in order to properly capture wall effects and flow detachment. Dimensionless distance y^+ goes from a range of 1 to 5 inside the orifice, to approximately 5 to 15 in the other walls of the domain. A sketch of the mesh topology can be seen in figure 1.b. I

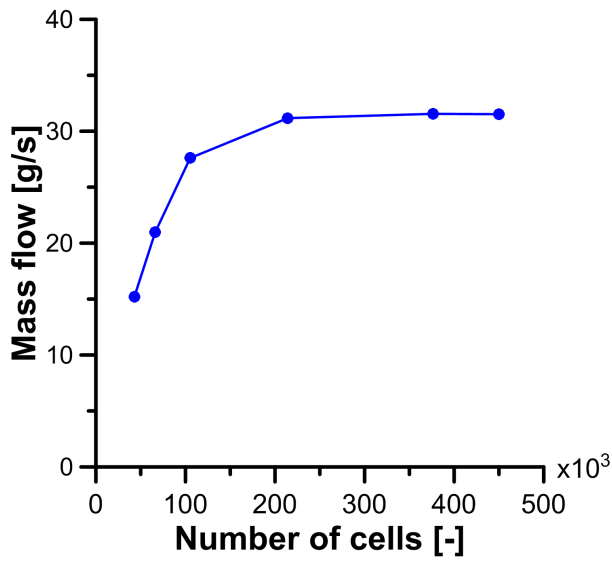

Figure 2. Mesh sensitivity study

All the geometries in the study represent a 6-hole nozzle. In order to reduce the computational effort, a sector-symmetric simulation representing only one of these 6 orifices has been calculated. This assumption can be assumed as reasonable for symmetric injectors operating at high needle lifts, where most of the flow comes from the needle seat region, and 3-dimensional phenomena appearing in the sac volume are less significant. As a consequence of this simplification, symmetry-plane boundary conditions are used in the lateral planes. A fixed pressure condition is used for the inlet section of the nozzle. For the orifice outlet, a mean pressure boundary condition has been selected

in order to allow low-pressure values associated to the eventual arrival of cavitation to the outlet section. For all the walls, a non-slip condition is selected for the velocity.

During the simulations, 3 levels of injection pressure (40, 120 and 200 MPa) are calculated, with up to 13 values of backpressure in a range from 0.1 to 12 MPa. This has been done in order to properly study the eventual transition from cavitating to non-cavitating regime inside the nozzle orifices.

Validation

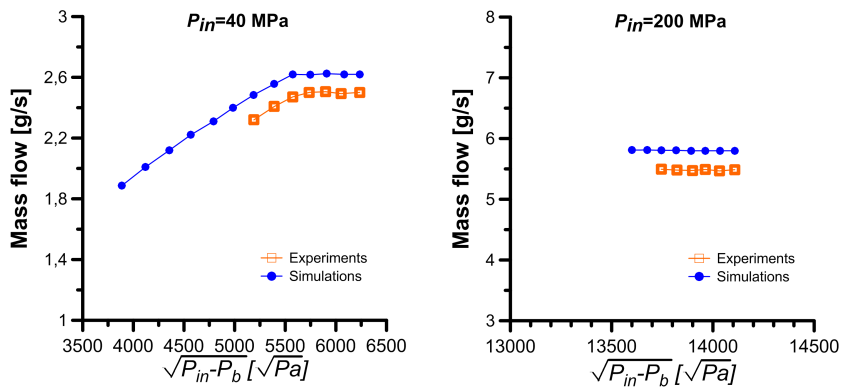

Figure 3. Comparison of experiments vs. simulation results

The current simulation arrangement has been validated against experimental mass flow measurements for the cylindrical geometry in Figure 3. As it can be seen, the CFD methodology is able to capture the overall behavior of the mass flow for both low (40 MPa) and high (200 MPa) injection pressures, with a maximum deviation of approximately 5%. This deviation can be explained in terms of small uncertainties in the nozzle geometry determination (especially in aspects like the inlet rounding radii or the surface finish quality), as well as potential changes of the liquid properties due to compressibility or thermal effects, which are not currently considered. Additionally, in the case of $P_{in} = 40MPa$, the model is able to properly reproduce the transition point where mass flow choking induced by cavitation appears.

Results

Hydraulic characteristics

Figure 4 shows the results from all the calculations against the square root of the pressure difference between the injection pressure (P_{in}) and the backpressure P_b. In this figure, each cloud of points corresponds to a level of injection pressure, while different symbols are used for each nozzle geometry.

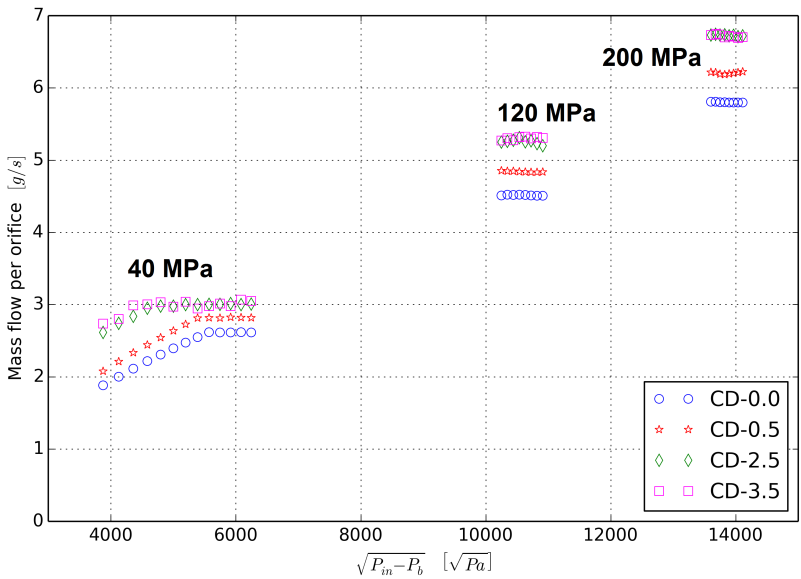

Figure 4. Evolution of outlet mass flow rate vs. $\sqrt{P_{in} - P_b}$.

Looking at the results from the cylindrical nozzle (CD-0.0, in circle symbols) and an injection pressure of 40 MPa, two distinctive regions can be identified. For low $\Delta P = P_{in} - P_b$ values (i.e., high P_b), the mass flow out of the nozzle grows linearly with the square root of this pressure difference. At a certain backpressure value (called critical condition), the mass flow collapses in a single value. This behavior is associated in the literature with the appearance of cavitation [15;34;39].

Comparing the results of the different nozzles at this same 40 MPa injection pressure level, two main conclusions can be drawn. First, that the higher the conicity of the orifices, the larger the amount of flow delivered. This is due to the way the orifice geometries are constructed. As stated before, the nozzles are constructed so that the value

in the throttle section is equal for all the nozzles. This means that the outlet diameter of the orifice grows together with its $k-factor$. The other important aspect is that the geometries with higher $k-factor$ are also more prone to cavitate, since the critical condition is achieved at smaller $P_{in}-P_b$ values. This is contrary to what occurs with standard convergent nozzles, where higher degrees of conicity imply less probability to cavitate.

When injection pressure increases (120, 200 MPa), all the geometries show cavitating behavior in the mass flow rate for all the backpressure values simulated. The only difference noticed among the nozzles is regarding the mass flow value, which is linked to the outlet diameter, as previously stated.

Figure 5 shows the void fraction fields inside the nozzle for two different operating conditions. For each nozzle and condition, two planes have been represented: one corresponding to the transverse section at the middle of the orifice, and another perpendicular to it.

The condition at the left hand side ($P_{in}=40MPa-P_b=9MPa$) corresponds to a backpressure slightly lower than the critical conditions for the cylindrical nozzle (CD-0.0). On the right hand side, a condition of extreme cavitation ($P_{in}=200MPa-P_b=1MPa$) is represented. It can be observed that the region where cavitation is produced depends on the specific orifice geometry:

- Cylindrical nozzle (CD-0.0). In this case, it can be seen that cavitation starts forming at the upper side of the orifice inlet, as a consequence of the flow bending from the needle seat section. As the conditions become more favorable to cavitation, the area occupied by the vapor enlarges, reaching the orifice outlet.
- Low-conicity nozzle (CD-0.5). The small level of conicity helps to reduce the length and intensity of the cavitation region, but the overall flow characteristics remain very similar to the cylindrical nozzle.
- High conicity nozzles (CD-2.5 & CD-3.5). The cavitation formation at the orifice inlet disappears, which is consistent with observations available in the literature for convergent nozzles[15;34]. Nevertheless, cavitation is now induced close to the throttle section, between the convergent and the divergent portions of the orifice. At this point, creating the low-pressure conditions that are responsible for hydrodynamic cavitation occurrence. This new cavitation region is the one responsible for the mass flow collapse observed in figure 4 for the high $k-factor$ geometries. The intensity of this flow separation and consequent cavitation formation is generally more intense in the bottom side of the orifice. This can be

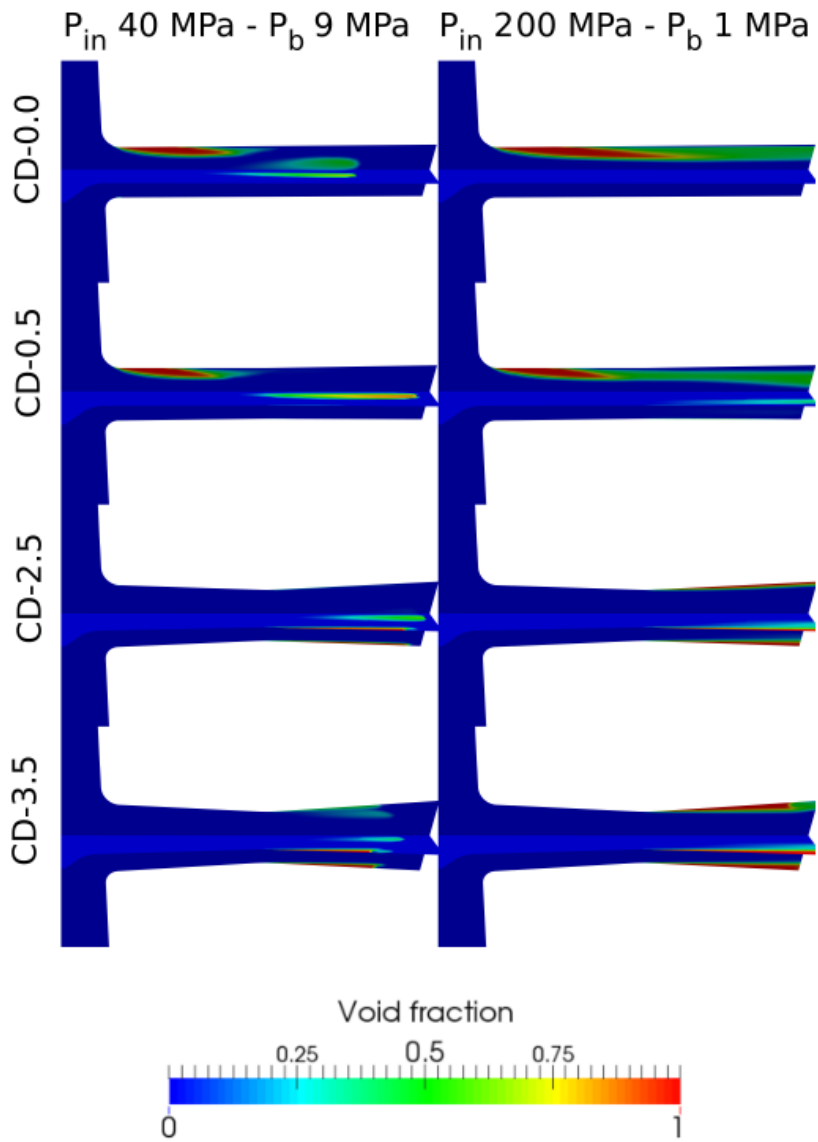

Figure 5. Void fraction distribution fields inside the nozzles. Left: $P_{in} = 40MPa - P_b = 9MPa$; right: $P_{in} = 200MPa - P_b = 1MPa$;.

observed from the CD-2.5 orifice results, where no cavitation can be detected in

the upper side, while the bottom and middle sections show significant cavitation formation.

This behavior is more clearly seen in Figure 6, where the liquid flow velocity vectors are depicted for the $P_{in} = 200MPa - P_b = 1MPa$ condition. In the case of the cylindrical nozzle, the vectors show a recirculation zone (low velocity area) in the upper section of the orifice inlet, which is linked to the cavitation formation previously observed. In the rest of the orifice, and in particular close to its outlet, most of the flow is parallel to the orifice axis.

In the case of the high conicity nozzle (CD-3.5), the recirculation areas can be identified starting from the throttle section, with higher intensity at the bottom side, which explains the results obtained in terms of void fraction. This is due to the fact that the inlet upper corner creates some level of flow separation, similar to what has been discussed for the cylindrical nozzle, but to a lower extent. As a consequence of this separation, the flow arrives to the bottom of the throttle section in a less structured fashion, slightly reducing the intensity of the recirculation after the throttle. At the outlet section, the core of the flow occupies the central area of the orifice, although the flow starts showing some tendency to also reach the external sides of the orifice.

The same results are depicted in terms of the nozzle discharge coefficient in Figure 7. What can be observed is that the cylindrical and low $k - factor$ nozzles (CD0.0 and CD0.5) are characterized by a high discharge coefficient (around 0.93) for the conditions at which cavitation does not take place. When the ΔP increases, mass flow collapse induced by cavitation appears, and as a consequence the discharge coefficient drops significantly.

The nozzles with higher $k - factor$ (CD2.5 and CD3.5) are generally showing lower discharge coefficient compared to the low $k - factor$ ones. This behavior is due to two phenomena. On the one hand, the recirculation zones appearing in the throttle section are the source for a pressure drop inside the orifice, which is not appearing on the low $k - factor$ cases. On the other hand, the higher intensity of cavitation already seen for these nozzles, and the mass flow rate collapse associated to it, further reduces the nozzle flow capability.

One important parameter for the spray atomization and mixing processes is the effective velocity at the nozzle outlet (u_{eff}). This parameter can be obtained as the ratio between the integrated momentum flux and mass flow rate at the nozzle outlet:

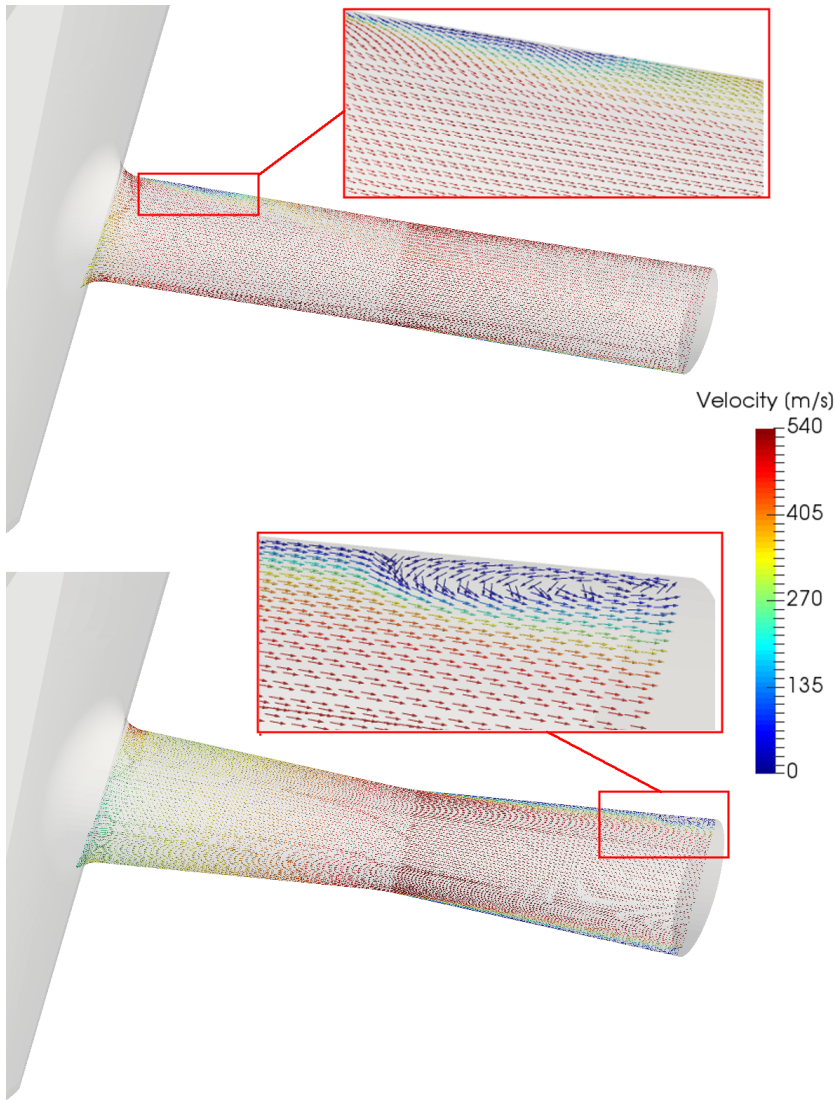

Figure 6. Flow velocity vectors for nozzles CD-0.0 (top) and CD-3.5 (bottom). $P_{in} = 200MPa - P_b = 1MPa$;.

$$u_{eff} = \frac{\dot{M}_o}{\dot{m}_o} = \frac{\rho_l A_{eff} u_{eff}^2}{\rho_l A_{eff} u_{eff}} \tag{7}$$

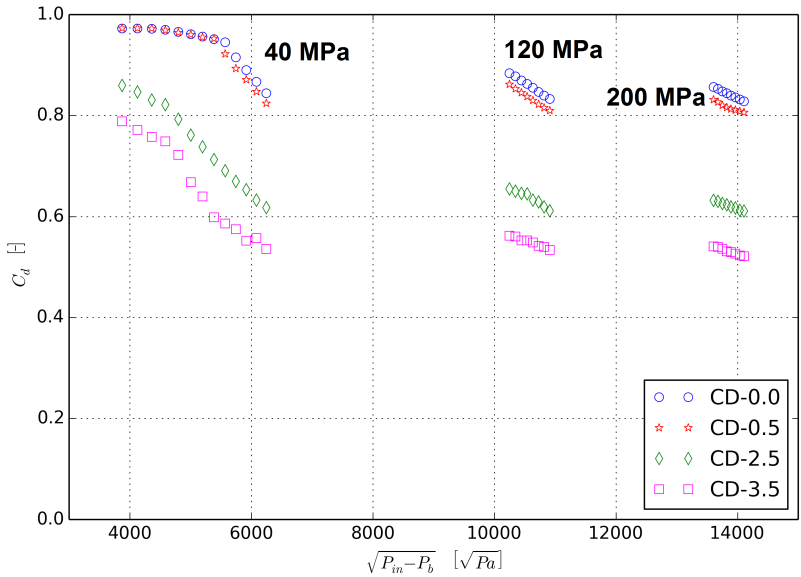

Figure 7. Evolution of nozzle discharge coefficient vs. $\sqrt{P_{in} - P_b}$.

Figure 8 depicts this effective velocity against the square root of the pressure difference ΔP for a 40 MPa injection pressure. For low values of ΔP, the nozzles with higher conicity exhibit lower values of effective velocity. This behavior is due to the effect of the divergent section, which acts as a diffuser, reducing the local velocity fields. Nevertheless, as the pressure difference increases, the cavitation region observed after the throttle section for the convergent-divergent nozzles virtually confines the core of the flow into the central section, and the effective velocity values become more and more similar to those observed for the cylindrical nozzle. The same kind of behavior can be observed in Figure 9 for 200 MPa injection pressure, where effective outlet velocity even becomes slightly higher for the highest conicity nozzle.

Figure 10 shows the values of the area coeficient C_a as a function of the square root of ΔP. The area coefficient can be calculated from the effective velocity and the discharge coefficient using the following relationships:

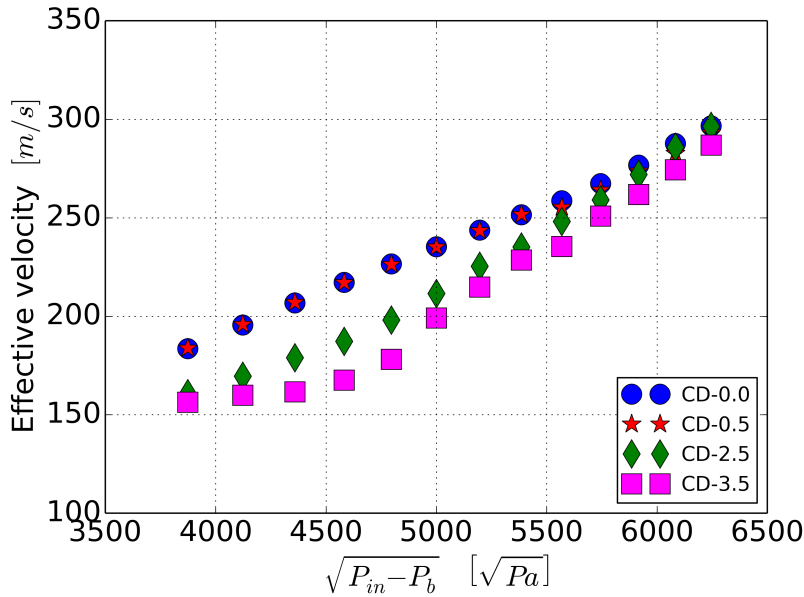

Figure 8. Evolution of effective velocity vs. $\sqrt{P_{in} - P_b}$. $P_{in} = 40MPa$

$$C_d = C_v \cdot C_a \tag{8}$$

$$C_v = \frac{u_{eff}}{u_{th}} \tag{9}$$

$$u_{th} = \sqrt{\frac{2 \cdot \Delta P}{\rho_l}} \tag{10}$$

It can be seen in the figure that for all nozzles the area coefficient is close to the unity when cavitation does not take place. Then, as cavitation builds up, there is a portion of the outlet section that is not properly used for fuel delivery due to the presence of cavitation bubbles, and C_a drops significantly. Since higher conicity nozzles start showing cavitation phenomena for lower ΔP, the drop in C_a is more appreciable. Nevertheless, it seems that the decreasing slope of C_a vs $\sqrt{\Delta P}$ is similar for all nozzles. This indicates that the area coefficient decrease is related to the amount of vapor that is formed inside the nozzle, and not so much to its spacial distribution inside it.

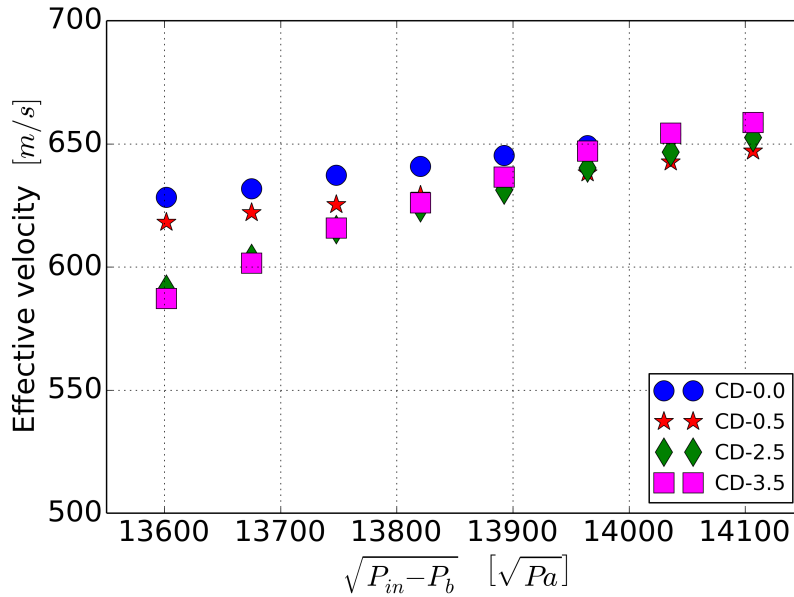

Figure 9. Evolution of effective velocity vs. $\sqrt{P_{in} - P_b}$. $P_{in} = 200MPa$

In the $P_{in} = 200MPa$ case, the conditions are such that cavitation reaches the nozzle outlet for any backpressure value, and the influence of P_b on the area coefficient becomes almost negligible. In this case, there is a perfect scaling with the orifice $k - factor$.

Considerations on spray characteristics

From the internal nozzle flow CFD results, the hydraulic behavior of convergent-divergent nozzles can be summarized as follows:

- Flow separation at the throttle section, inducing cavitation formation in this region at lower ΔP values compared to the cylindrical nozzle. As a consequence, the amount of vapor formed at the same pressure conditions is higher for this kind of nozzle.
- Lower stationary discharge coefficient, induced by the flow separation and the higher intensity of cavitation.
- Equivalent effective outlet velocities if the pressure drop along the orifice is sufficiently high, since the diffusive effect of the nozzle geometry is compensated by the increase induced by the more significant appearance of cavitation.

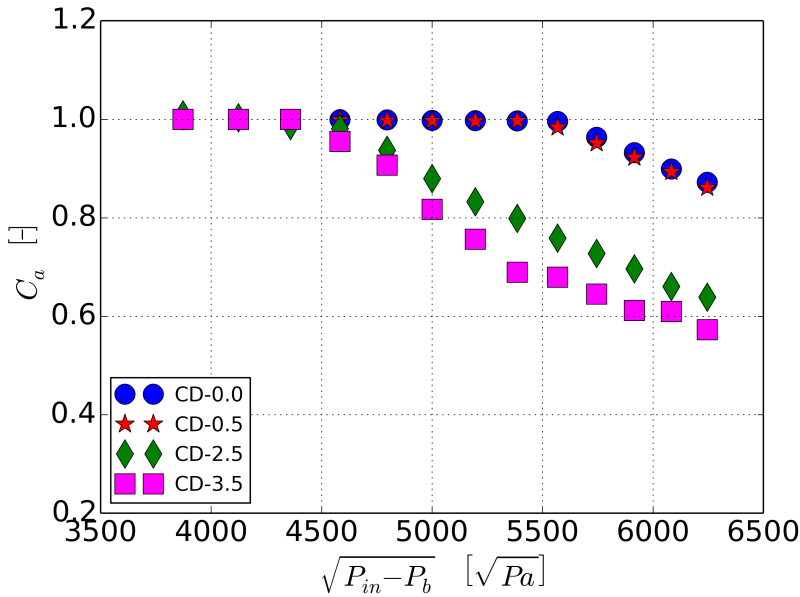

Figure 10. Evolution of the area coefficient vs. $\sqrt{P_{in} - P_b}$. $P_{in} = 40MPa$

Taking into account these flow characteristics, the sprays originated from convergent-divergent nozzles are expected to have the following characteristics compared to cylindrical nozzles:

- Equivalent or more efficient spray atomization, as a consequence of the combination of similar outlet velocities and higher cavitation intensity, which is known to improve atomization due to the flow disruption originated when the cavitation bubbles collapse at the outlet orifice [19;42].
- Wider spray opening angle (better fuel-air mixing), as a consequence of the radial velocity component associated to the divergent section plus the effect of cavitation, which is also known to increase spray opening angles [19;20;37]
- Reduced spray liquid length and lower overall local equivalence ratios, with potential for soot formation reduction.

With all considered, convergent-divergent nozzles show some potential advantages in spray formation and mixing processes. Nevertheless, these aspects need to be further investigated and eventually confirmed with experimental spray combustion visualization tests.

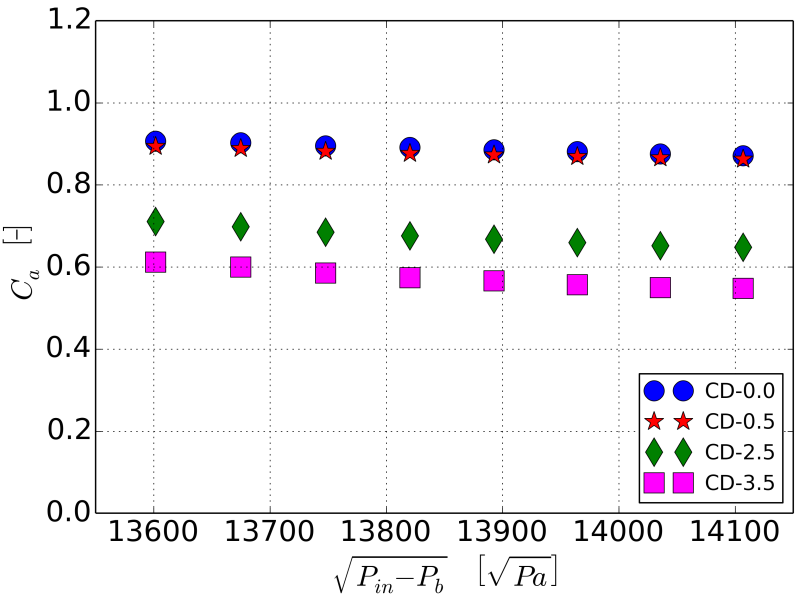

Figure 11. Evolution of the area coefficient vs. $\sqrt{P_{in} - P_b}$. $P_{in} = 200MPa$

Conclusions

In the current paper, a computational investigation of the hydraulic performance of diesel nozzles with convergent-divergent orifices has been performed. For this purpose, a Homogeneous Equilibrium Model (HEM), implemented in OpenFoam, has been used to predict cavitation formation.

The main conclusions from this investigation are:

- Mass flow rate collapse induced by cavitation in convergent-divergent nozzles appears at lower ΔP values compared to an equivalent cylindrical nozzle. This is opposite to the behavior observed in the literature from purely convergent nozzles, where mass flow collapse induced by cavitation is delayed or even totally inhibited.
- Cylindrical nozzles and convergent-divergent nozzles with low $k - factor$ show cavitation formation at the orifice inlet, generated by the bent induced when the flow passes from the needle seat area to the orifice. High $k - factor$ convergent-divergent nozzles do not present cavitation in this area, as it would be expected from the experience with convergent nozzles. Nevertheless, a flow separation region appears at the transition between the convergent and divergent portions of

the orifice. This flow separation is the responsible for the cavitation formation in convergent-divergent nozzles, and the subsequent mass flow collapse.

- Effective outlet velocity of convergent-divergent nozzles is smaller at low ΔP values, due to the effect of the divergent section. Nevertheless, when ΔP gets higher and cavitation intensity increases, there is an associated velocity increase, reaching equivalent or even higher effective velocities than the cylindrical nozzle for the high $k - factor$ cases.
- Effective outlet area is close to the unity for all the nozzles when cavitation does not take place, dropping significantly when it appears. The slope of this decrease against $\sqrt{\Delta P}$ is similar for the cylindrical and the convergent-divergent nozzles, showing that this parameter is more sensitive to the amount of cavitation formed than to the location of this cavitation.
- From the hydraulic behavior of these nozzles, equivalent or better spray atomization efficiency and lower liquid length can be expected from convergent-divergent nozzles compared to cylindrical nozzles. This is due to the combination of the equivalent outlet velocities, the higher radial velocity component at the outlet orifices provided by the divergent section and the higher cavitation intensity, increasing both atomization efficiency and spray opening angle.

Acknowledgments

This work was partly sponsored by "Ministerio de Economía y Competitividad", of the Spanish Government, in the frame of the Project "Estudio de la interacción chorro-pared en condiciones realistas de motor", Reference TRA2015-67679-c2-1-R.

The authors would like to thank the computer resources, technical expertise and assistance provided by the Universidad de Valencia in the use of the supercomputer "Tirant".

References

1. J. M. Lujan, B. Tormos, F. J. Salvador, K. Gargar, Comparative analysis of a DI diesel engine fuelled with biodiesel blends during the European MVEG-A cycle: Preliminary study (I), Biomass and Bioenergy 33 (6-7) (2009) 941–947. doi:10.1016/j.biombioe.2009.02.004.

2. B. Guan, R. Zhan, H. Lin, Z. Huang, Review of state of the art technologies of selective catalytic reduction of NOx from diesel engine exhaust, Applied Thermal Engineering 66 (1-2) (2014) 395–414. doi:10.1016/j.applthermaleng.2014.02.021.
3. C. A. Idicheria, L. M. Pickett, Ignition, soot formation and end-of-combustion transients in diesel combustion under high-EGR conditions, Internation Journal of Engine Research 12 (2011) 1–17. doi:10.1177/1468087411399505.
4. R. Kiplimo, E. Tomita, N. Kawahara, S. Yokobe, Effects of spray impingement, injection parameters and EGR on the combustion and emission characteristics of a PCCI diesel engine, Applied Thermal Engineering 37 (2012) 165–175. doi:10.1016/j.applthermaleng.2011.11.011.
5. V. Gopalakrishnan, A. Vassallo, R. C. Peterson, J. De la Morena, Effect of high levels of boost and recirculated exhaust gas on diesel combustion characteristics at part load, SAE Technical Papers 2014-01-1245.doi:10.4271/2014-01-1245.
6. F. J. Salvador, S. Ruiz, J. Gimeno, J. De la Morena, Estimation of a suitable Schmidt number range in diesel sprays at high injection pressure, International Journal of Thermal Sciences 50 (9) (2011) 1790–1798. doi:10.1016/j.ijthermalsci.2011.03.030.
7. H. Chaves, C. Kirmse, F. Obermeier, Velocity measurements of dense diesel fuel sprays in dense air, Atomization and sprays 14 (6) (2004) 589–609.
8. J. M. Desantes, F. J. Salvador, J. J. Lopez, J. De la Morena, Study of mass and momentum transfer in diesel sprays based on X-ray mass distribution measurements and on a theoretical derivation, Experiments in Fluids 50 (2) (2011) 233–246. doi:10.1007/s00348-010-0919-8.
9. X. Wang, Z. Han, W. Su A numerical study of the effects of pressure fluctuations inside injection nozzle on high-pressure and evaporating diesel spray characteristics, Applied Mathematical Modelling 40 (2016) 4032–4043. newblock doi:10.1016/j.apm.2015.11.014.
10. F. J. Salvador,J. Gimeno, J. De la Morena, M. CarreresUsing one-dimensional modeling to analyze the influence of the use of biodiesels on the dynamic behavior of solenoid-operated injectors in common rail systems: Results of the simulations and discussion, Energy Conversion and Management 54 (2012) 122–132. doi:10.1016/j.enconman.2011.10.007.
11. P. K. Karra, S.-C. Kong, Experimental Study on Effects of Nozzle Hole Geometry on Achieving Low Diesel Engine Emissions, Journal of Engineering for Gas Turbines and Power 132 (2) (2010) 022802. doi:10.1115/1.3124791.

12. R. Payri, F. J. Salvador, J. Gimeno, J. De la Morena, Effects of nozzle geometry on direct injection diesel engine combustion process, Applied Thermal Engineering 29 (10) (2009) 2051–2060. doi:10.1016/j.applthermaleng.2008.10.009.
13. S. Som, A. I. Ramirez, D. E. Longman, S. K. Aggarwal, Effect of nozzle orifice geometry on spray, combustion, and emission characteristics under diesel engine conditions, Fuel 90 (3) (2011) 1267–1276. doi:10.1016/j.fuel.2010.10.048.
14. A. Zhang, A. Montanaro, L. Allocca, J. Naber, S.-Y. Lee, Measurement of Diesel Spray Formation and Combustion upon Different Nozzle Geometry using Hybrid Imaging Technique, SAE Technical Paper 2014-01-1410.doi:10.4271/2014-01-1410.
15. D. P. Schmidt, M. L. Corradini, The internal flow of Diesel fuel injector nozzles: a review, Int J Engine Research. JER 00201 ImechE 2 (6) (2001) 1–22. doi:10.1243/1468087011545316.
16. S. Som, D. Longman, A. Ramirez, S. Aggarwal, Influence of Nozzle Orifice Geometry and Fuel Properties on Flow and Cavitation Characteristics of a Diesel Injector, in: Fuel Injection in Automotive Engineering, 2012, pp. 112–126. doi:10.5772/38900.
17. R. Payri, F. J. Salvador, J. Gimeno, R. Novella, Flow regime effects on non-cavitating injection nozzles over spray behavior, International Journal of Heat and Fluid Flow 32 (2011) 273–284. doi:10.1016/j.ijheatfluidflow.2010.10.0.
18. J. J. Lopez, F. J. Salvador, O. De la Garza, J. Arregle, A comprehensive study on the effect of cavitation on injection velocity in diesel nozzles, Energy Conversion and Management 64 (2012) 415–423. doi:10.1016/j.enconman.2012.03.032.
19. J. M. Desantes, R. Payri, F. J. Salvador, J. De la Morena, Influence of cavitation phenomenon on primary break-up and spray behavior at stationary conditions, Fuel 89 (10) (2010) 3033–3041. doi:10.1016/j.fuel.2010.06.004.
20. A. Andriotis, M. Gavaises, Influence of vortex flow and cavitation on near-nozzle diesel spray dispersion angle, Atomization and Sprays 19 (3) (2009) 247–261.
21. Z. Liu, K.-S. Im, Y. Wang, K. Fezzaa, J. Wang, X.-B. Xie, M.-C. Lai, Near-Nozzle Structure of Diesel Sprays Affected by Internal Geometry of Injector Nozzle: Visualized by Single-Shot X-ray Imaging, SAE Technical Paper 2010-01-0877 (2010). doi:10.4271/2010-01-0877.
22. F. J. Salvador, M. Carreres, D. Jaramillo, J. Martínez-López, Comparison of microsac and VCO diesel injector nozzles in terms of internal nozzle flow characteristics, Energy Conversion and Management 103 (2015) 284–299. doi:10.1016/j.enconman.2015.05.062.

23. N. Mitroglou, M. McLorn, M. Gavaises, C. Soteriou, M. Winterbourne, Instantaneous and ensemble average cavitation structures in Diesel micro-channel flow orifices, Fuel 116 (2014) 736–742. doi:10.1016/j.fuel.2013.08.060.
24. R. Payri, F. J. Salvador, J. Gimeno, O. Venegas, Study of cavitation phenomenon using different fuels in a transparent nozzle by hydraulic characterization and visualization, Experimental Thermal and Fluid Science 44 (2013) 235–244. doi:10.1016/j.expthermflusci.2012.06.013.
25. W. Zhong, Z. He, Q. Wang, Z. Shao, X. Tao, Experimental study of flow regime characteristics in diesel multi-hole nozzles with different structures and enlarged scales, International Communications in Heat and Mass Transfer 59 (2014) 1–10. doi:10.1016/j.icheatmasstransfer.2014.10.001.
26. A. Sou, R. H. Pratama, R. Ohashi, R. Sugimura, Cavitation in a nozzle with asymmetric inflow and its effects on liquid jet, ILASS - Europe 2011.
27. B. Biçer, A. Sou, Application of the improved cavitation model to turbulent cavitating flow in fuel injector nozzle, Applied Mathematical Modelling 40 (2016) 4712–4726. newblock doi:10.1016/j.apm.2015.11.049.
28. L. C. Ganippa, G. Bark, S. Andersson, J. Chomiak, Comparison of cavitation phenomena in transparent scaled-up single-hole Diesel nozzles, in: Symposium on Cavitation, 2001, pp. 1–9.
29. J. De la Morena, K. Neroorkar, A. H. Plazas, R. C. Peterson, D. P. Schmidt, Numerical analysis of the influence of diesel nozzle design on internal flow characteristics for 2-valve diesel engine application, Atomization and Sprays 23 (2) (2013) 97–118. doi:10.1615/AtomizSpr.2013006361.
30. C. Habchi, N. Dumont, O. Simonin, Multidimensional simulation of cavitating flows in Diesel injectors by a homogeneous mixture modeling approach., Atomization and Sprays 18 (2014) 129–162.
31. F. J. Salvador, J. Martínez-López, M. Caballer, C. De Alfonso, Study of the influence of the needle lift on the internal flow and cavitation phenomenon in diesel injector nozzles by CFD using RANS methods, Energy Conversion and Management 66 (2013) 246–256. doi:10.1016/j.enconman.2012.10.011.
32. W. Ning, R. D. Reitz, R. Diwakar, A. M. Lippert, A Numerical Investigation of Nozzle Geometry and Injection Condition Effects on Diesel Fuel Injector Flow Physics, SAE Technical Paper 2008-01-0936.doi:10.4271/2008-01-0936.
33. F. J. Salvador, M. Carreres, D. Jaramillo, J. Martínez-lópez, Analysis of the combined effect of hydrogrinding process and inclination angle on hydraulic performance of diesel injection nozzles, Energy Conversion and Management 105 (2015) 1352–1365. doi:10.1016/j.

enconman.2015.08.035.

34. F. Payri, R. Payri, F. Salvador, J. Martínez-López, A contribution to the understanding of cavitation effects in Diesel injector nozzles through a combined experimental and computational investigation, Computers & Fluids 58 (2012) 88–101. doi:10.1016/j.compfluid.2012.01.005.
35. O. O. Taskiran, M. Ergeneman, Effect of nozzle dimensions and fuel type on flame lift-off length, Fuel 115 (2014) 833–840. doi:10.1016/j.fuel.2013.03.005.
36. B. Mohan, W. Yang, S. K. Chou, Cavitation in Injector Nozzle Holes - A Parametric Study, Engineering Applications of Computational Fluid Mechanics 8 (1) (2014) 70–81.
37. F. J. Salvador, J. V. Romero, M. D. Roselló, J. Martínez-López, Validation of a code for modeling cavitation phenomena in Diesel injector nozzles., Mathematical and Computer Modelling 52 (7-8) (2010) 1123–1132. doi:10.1016/j.mcm.2010.02.027.
38. F. J. Salvador, S. Hoyas, R. Novella, J. Martinez-Lopez, Numerical simulation and extended validation of two-phase compressible flow in diesel injector nozzles, Proceedings of the Institution of Mechanical Engineers, Part D: Journal of Automobile Engineering 225 (4) (2011) 545–563. doi:10.1177/09544070JAUTO1569.
39. F. J. Salvador, J. Martínez-López, J. V. Romero, M. D. Roselló, Computational study of the cavitation phenomenon and its interaction with the turbulence developed in diesel injector nozzles by Large Eddy Simulation (LES), Mathematical and Computer Modelling 57 (7-8) (2013) 1656–1662. doi:10.1016/j.mcm.2011.10.050.
40. S. Molina, F. J. Salvador, M. Carreres, D. Jaramillo, A computational investigation on the influence of the use of elliptical orifices on the inner nozzle flow and cavitation development in diesel injector nozzles, Energy Conversion and Management 79 (2014) 114–127. doi:10.1016/j.enconman.2013.12.015.
41. J. M. Desantes, F. J. Salvador, M. Carreres, D. Jaramillo, Large-eddy simulation analysis of the influence of the needle lift on the cavitation in diesel injector nozzles, Proceedings of the Institution of Mechanical Engineers, Part D: Journal of Automobile Engineering 229 (4) (2015) 407–423. doi:10.1177/0954407014542627.
42. C. Dumouchel, On the experimental investigation on primary atomization of liquid streams, Experiments in Fluids 45 (3) (2008) 371–422. doi:10.1007/s00348-008-0526-0.